



Quantitative Characterization of the Perforation Behaviour of Direct Recycled Aluminum Alloy 6061 Plates Subjected to High-Velocity Impact

Irfan Alias Farhan Latif¹, Mohd Khir Mohd Nor^{1,2,*}, Nur Kamilah Yusuf², S Kanna Subramanian¹, Mohd Syazwan Abdul Samad³, Norzarina Ma'at¹

¹ Crashworthiness and Collisions Research Group (COLORED), Faculty of Mechanical and Manufacturing Engineering, Universiti Tun Hussein Onn Malaysia, Parit Raja, Johor, Malaysia

² Advanced Materials and Manufacturing Centre (AMMC), Institute for Integrated Engineering (I²E), Universiti Tun Hussein Onn Malaysia, Parit Raja, Johor, Malaysia

³ Package Design Engineering, Package Technology Development and Integration, Western Digital Corporation, Penang, Malaysia

ARTICLE INFO

Article history:

Received 4 March 2024

Received in revised form 30 April 2024

Accepted 14 May 2024

Available online 30 May 2024

Keywords:

Direct recycling; aluminum alloy 6061; high velocity impact; perforation behaviour

ABSTRACT

This study aims to establish the perforation behaviour of direct recycled AA6061 to help establish the properties of the current most optimized direct recycled AA6061 through the hot press forging technique. This was achieved by subjecting direct recycled AA6061 plates of varying thickness to high-velocity impacts using a single-stage gas gun setup. The impactor is a hemispherical steel projectile of 13mm in length and 8.5mm in diameter. Plates of 3,4,5 and 10mm thickness were tested at velocities ranging from 120 m/s to 402 m/s. The deformation profiles of the impacted plates were captured and analyzed to quantitatively establish the perforation behaviour of recycled AA6061 plates. The plates showed irregular and non-axis symmetric patterns of deformation hinting the material exhibits anisotropic properties. The changes in the deformation profile were investigated in relation to changes in impact velocities and plate thickness were made to understand how they impact the profile. The deformation area was observed to be decreasing when the bullet impact velocity was increased. Higher velocity impact events lead to more material ejection from the plate in the form of fragmentation. Additionally, the deformation zone was observed to be getting smaller with an increase in the thickness of the plate. Thicker plates were found to have more fragmentation compared to thinner plates. Ductile failure characteristics such as petal formation and plugging were observed along with brittle characteristics such as fragmentation and conal fractures. Lower-velocity impacts lead to more energy absorbed by the target plates. Thicker plates observed more of the bullet's energy. Through experimentation, the deformation behaviour of the directly recycled AA6061 material was established. This data can be used as a base for further research into the material's behaviour characterisation.

* Corresponding author.

E-mail address: khir@uthm.edu.my

<https://doi.org/10.37934/aram.118.1.193211>

1. Introduction

Aluminum is a lightweight metal with excellent properties that are used in major aspects of modern society such as defence, transportation, packaging, and energy industries [1,2]. The demand for aluminum has been consistently high and continues to increase over time. Since the year 2000, global aluminum production has increased by 250%. In 2018, the demand reached an estimated 65 million metric tons per year. By the year 2040, global aluminum demand is projected to continue to grow, to as much as 90 million tons per year [3]. However, aluminum refining process incurs some undesirable consequences in the form of CO² and GHG emissions [4]. These emissions are accountable for about 2% of the annual global CO² and GHG emissions due to human activities [5]. Under these circumstances, meeting the projected increase in demand simply by increasing aluminum production is not an ideal solution as it will certainly increase the global CO² and GHG emissions.

It is generally agreed that recycling is a suitable approach for aluminum as it possesses good recyclability at the end of its life cycle with the potential of retaining about 90% of the material used [6]. This is a promising idea since about 75% of the recorded aluminum production is still in circulation [6]. Aluminum recycling is by no means a new idea. It has been in practice ever since the age of industrialization in the 1900s. However, aluminum recycling comes with its own set of complications. For instance, the conventional recycling approach of melting and re forging the material incurs heavy material losses as only about 55% of initial scrap material is deemed recoverable [7]. The conventional approach also leads to GHG emissions albeit at a much lower scale compared to primary aluminum refining. To mitigate the negative effects of the conventional recycling approach, direct recycling techniques are being considered as they allow recycling of the aluminum without melting the scrap, leading to the lowest amount of GHG emissions and material losses [8-14]. This direct recycling method was first introduced back in 1996 by Gronostajski, Marciniak & Matuszak [15,16].

One direct recycling technique that has become quite popular is hot press forging. This technique utilizes a forge consisting of a die and press to press the recycled material together using hydraulic pressure at temperatures approaching but not exceeding the melting point of the recycled material. Another good technique is hot extrusion which also has been utilized for recycling aluminum [17]. For this work, hot press forging is the technique of concern. For recycling aluminum, much work has been done using this technique. A sustainable direct recycling method of AA6061 chips using a hot press forging process has already been proposed and adopted in various works [8,12]. It was observed that the material properties can vary by a significant margin depending on the recycling parameters. These process parameters such as chip size, pre-compaction and holding times, operating temperature and pressure were optimized using response surface methodology (RSM) [12]. The specimen produced using the optimized parameters was found to have an ultimate tensile strength of around 250 MPa [18]. The elongation-to-failure percentage for recycled AA6061 is around 12% [18]. The material was also heat treated and it was observed that its tensile strength and microhardness significantly improved [19]. However, there is still room for further optimization of the recycling process [20]. In a recent investigation, it was observed the microstructure of recycled material has weaker chip bonds with plenty of voids and gaps present [9]. The tensile behaviour of the recycled AA6061 studied at temperatures of 100°C, 200°C and 300°C showed the flow stress of the material increased with increasing strain rate and decreased with increasing temperature [10], [21,22]. The same behaviour was observed in primary AA6061 and AA5083 [23,24]. In addition, at higher velocity impact, the data from Taylor cylinder impact tests showed that an anisotropic characteristic was retained and mild ductility deformation behaviour was confirmed [25]. The impact data at a higher strain rate was quite promising and impressive for recycled AA6061 formed using

the hot press forging technique even though mechanical properties degradation was found at a lower strain rate related to ductility. The same fracture modes were observed as shown by ductile materials undergoing the same loading condition.

Numerical analysis helps with material behaviour characterization by allowing the establishment of an extensive data bank without the need for experimentation [26]. Such models are present in literature for ductile materials such as the primary AA7010 and also for composites that behave in a brittle manner [27-30,43]. Using FEA, much more can be learned about the material in question such as its ballistic limit [31], oblique impact behaviour [32], ballistic response [33] and real life complex simulations [34] etc. However, to establish a numerical model, experimental data is required for validation [35]. This also applies to directly recycled AA6061 which is relatively a new material still and is missing some crucial data, especially for more complex models [36].

The primary AA6061 alloys are usually utilized in applications where they are expected to withstand high velocity impacts [37]. Therefore, it stands to reason that the recycled AA6061 should be given such attention as well. To establish the deformation behaviour of recycled aluminium alloys under high-velocity impact, further analysis related to impact resistance is required. Therefore, this study is conducted to critically investigate the perforation behaviour, deformation profile and critical perforation velocity of recycled plates of commercial aluminium alloy AA6061 produced using hot press forging. The plates are set to be hit by hemispherical steel bullets using a single-stage gas gun setup. Energy and velocity-related analyses are also carried out in this study.

2. Methodology

2.1 Test Setup

The test setup utilized in this study is a single-stage gas gun setup based on the NIJ-018.01 standard (National Institute of Justice, 1985). The entire gas gun setup arrangement is shown in Figure 1. The pressure vessel is the chamber where the gas that is used to propel the bullet is brought in and pressurized. The pressure valve mechanism helps to control the flow of gas. The breech is the point where the bullet is located in front of the gun barrel. After the gas reaches the desired pressure level, the pressure valve is opened and the bullet is carried through the gun barrel from the breech to the chamber box which holds the target plate. The target plate of an exposed area of 100mm x 100mm is placed in a jig fixture inside the chamber box. The holding plates are tightened by screws on both sides to keep the target in place during the impact event. Figure 2 shows a view of the chamber box where the target plates are positioned. A paper scale is placed in the chamber box along the path of the bullet to assist with velocity measurements. A high-speed camera is placed facing the chamber box to capture the impact event.

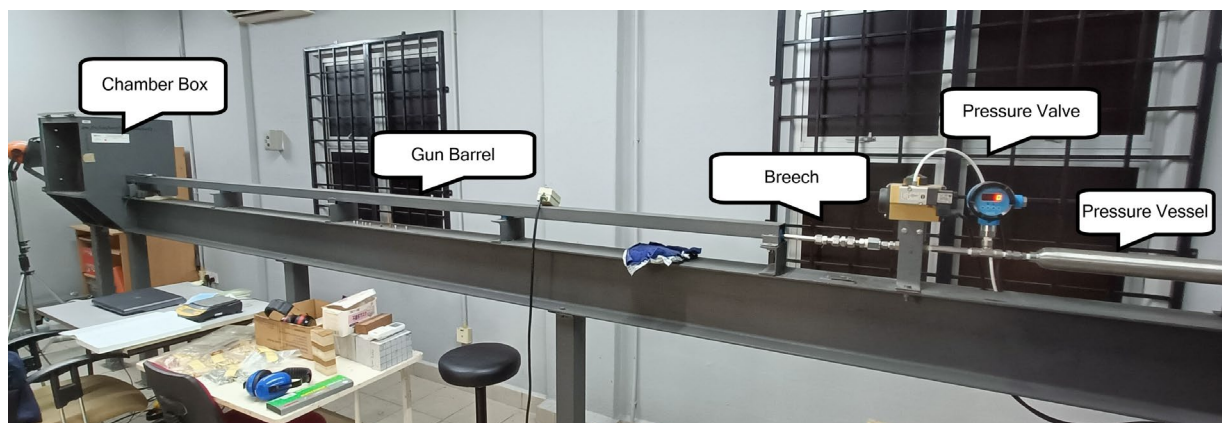


Fig. 1. The test setup

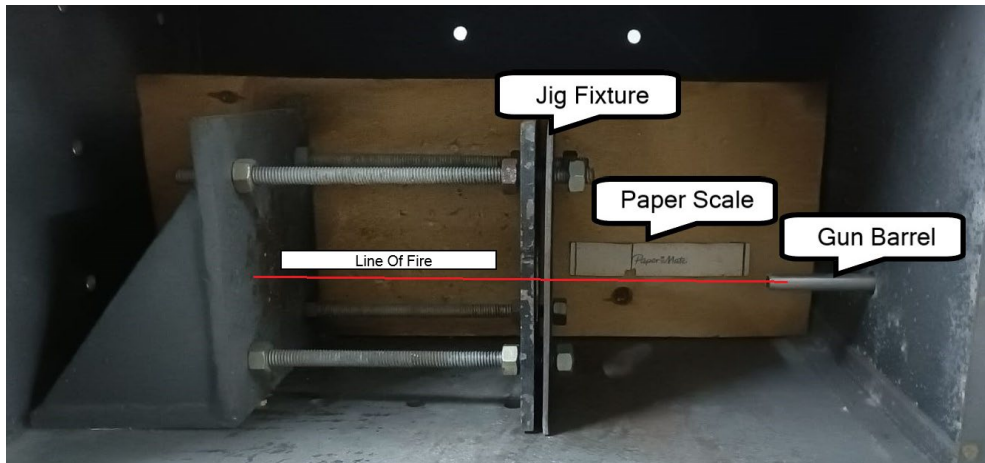


Fig. 2. Chamber box

The chosen projectile for the impact analysis is a hemispherical stainless-steel bullet of 13mm in length, 8.5mm in diameter and a mass of 5.3g. Helium gas is used to propel the projectile to its target. The highest-pressure level attainable by the pressure vessel is 150 bar which equates to a velocity of about 400 m/s. It should be noted that the actual velocity attained in each test event may vary. Figure 3 shows the impactor profile.



8.5mm diameter
Fig. 3. Projectile profile

2.2 Specimen Preparation

In accordance with the test setup, a 100mm x 100mm plate area of recycled AA6061 is prepared at 3, 4, 5 and 10mm thicknesses using the hot press forging technique. The process is shown in Figure 4, following the optimum setting in Table 1.

The preparation process starts with processing scrap into chips. The chips required for the recycled plates are produced using a CNC machine with an average rectangular shape of size 5.2mm x 1.097mm x 0.091 mm in length, width and thickness respectively. The CNC machine is run with a 10mm diameter tool with a feed rate of 0.05 mm/tooth, 1mm depth of cut and a cutting speed of

377m/min. The chips are collected and cleaned in an ultrasonic bath using acetone as the solution for 30 minutes. The chips are then dried in a thermal oven for 30 minutes at 60 °C. These parameters are optimized and adapted from previous research using the same preparation process [8].

After the chips are prepared, they are measured out to the required amount and placed in the mold and placed in the forge. Afterwards, the plate is taken out of the mold and is quenched in distilled water at a quench rate of 100°C/s. After quenching, the plate is placed in a thermal oven operating at a temperature of 175°C for 120 minutes. The resulting recycled plate is deemed to be T5-tempered.

Table 1
 Optimum operating parameters of the hot press forge [8]

Parameter	Value
Operating temperature	530°C
Operating pressure	47 MPa
Holding time	120 minutes
Compaction cycles	4
Compaction cycles duration	2 minutes

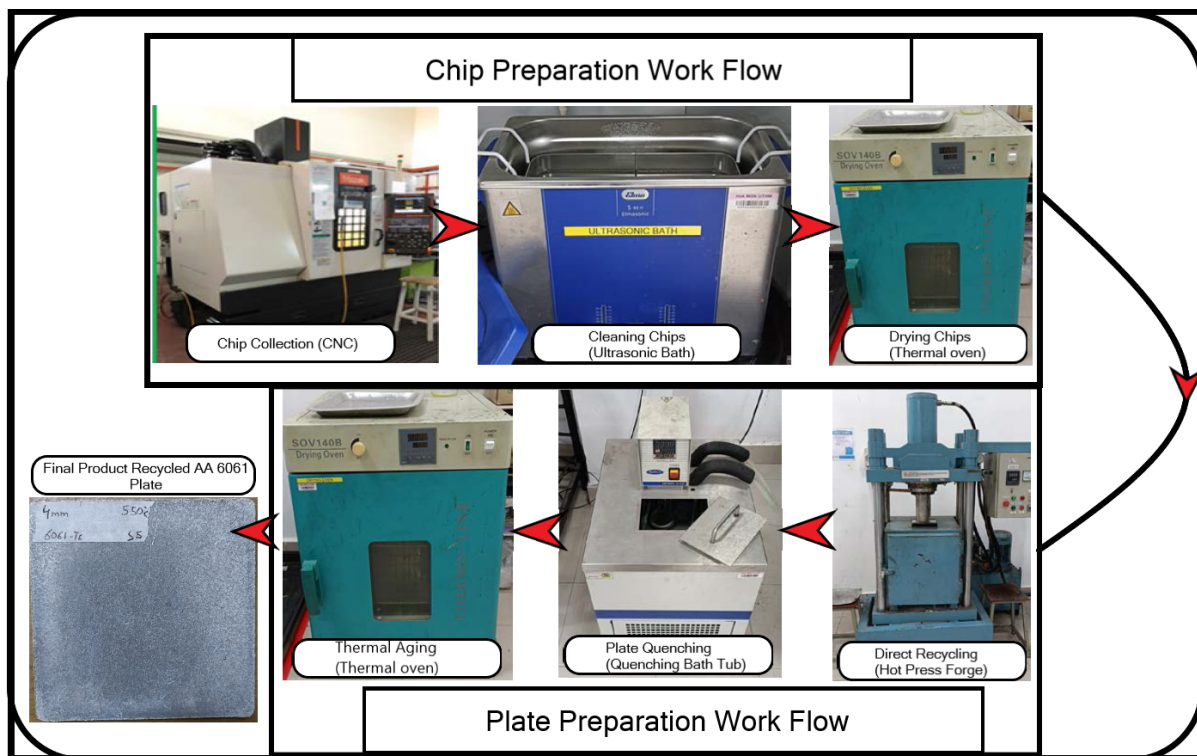


Fig. 4. Flow of specimen preparation [9]

2.3 Test Matrix

To get an appropriate range of impact velocity for the recycled AA6061 in this analysis, a few preliminary tests were conducted using the primary AA6061. Plates of 6mm and 10mm thicknesses were prepared and tested at a range of 100 to 400 m/s. It was observed that the 6mm plates experienced full penetration at a maximum velocity of 340 m/s and showed no penetration at 300 m/s. Whereas, the 10mm plate was not penetrated at the highest velocity. Bearing in mind that the

recycled form will exhibit lower impact resistance than its primary counterpart, the following experimental design is set in Table 2. For clarity, each test specimen is remarked uniquely.

Table 2

Experimental Test Matrix

Remark	Plate Thickness (mm)	Impact velocity (m/s)
R1	3	308
R2		333
R3		402
R4	4	121
R5		308
R6		402
R7	5	136
R8		308
R9	10	389

2.4 Data Analysis

After each successful impact test event, the target plate is carefully taken out of the chamber box and all of the resulting debris is collected. The general deformation of the plates is first captured, and followed by a 3D scanning to allow for a precision characterization of the deformed profile.

Additionally, the impact velocity and the residual velocity analysis are performed by gathering the respective values calculated using frame-by-frame analysis of the impact footage taken from the high-speed camera. The energy absorption capability of the plate is calculated by subtracting the kinetic energy of the bullet after impact from the kinetic energy of the bullet before impact [38]. Simply assuming that there is no energy loss, it can be said that the remaining energy is absorbed by the plate. The equation is shown below:

$$\frac{1}{2}mv_B^2 - \frac{1}{2}mv_A^2 = \text{Energy Absorbed By Plate} \quad (1)$$

Where ' m ' represents the mass of the bullet, ' v_B ' represents the velocity of the bullet before impact and ' v_A ' is the velocity of the bullet after impact (residual velocity).

3. Results and Discussion

As aforementioned, nine test settings are carried out in this study. All of them are characterized in terms of parameters such as bullet entry and exit hole areas, maximum plate deformation length, impact and residual velocities, and energy absorption of the plate. The following sections discuss the results of this test in further detail where the perforation behaviour of the deformed plates is carefully inspected and analysed.

3.1 Deformation Profile

In this section, the deformation profile of the direct-recycled AA6061 alloy plates subjected to high-velocity impact is quantitatively reported. An example of the deformation profile capturing is shown in Figure 5, while Table 3 shows the deformation configuration for all impact events. It can be seen from this table that the plates of recycled AA6061 do not result in a symmetrical deformation pattern which is normally connected to anisotropic behaviour. This behaviour is corroborated by C.S.

Ho when the recycled material was subjected to the Taylor cylinder impact test [9]. The deformation profile of the impact events shows irregular patterns which is similar to its primary counterpart AA6061. However, there are still a few deformed plates that show symmetry in at least one axis such as R1, R4, R7, and R9. The details of the deformation behaviour are configured in Table 4. All of the impact events resulted in full penetration of the target plates. Therefore, the deformation profile and the failure mechanism observed are only representative of the material's failure post-penetration. The material may exhibit a different behaviour leading up to penetration as the behaviour can vary depending on the strain rate induced on the material. In the observed impact events, the maximum displacement of the plate material along the direction of the plate varied from 1 to 15 mm. Bullet entry hole size ranges from 51 to 110 mm². As seen from the hole profile in Table 3, the variation is due to the bullet hitting the target plate at an angle. The deformation zone observed at the back of the plates varies from 399 mm² to 1693 mm². The details on how these variations relate to the impact velocity and plate thickness are discussed in the sections below.

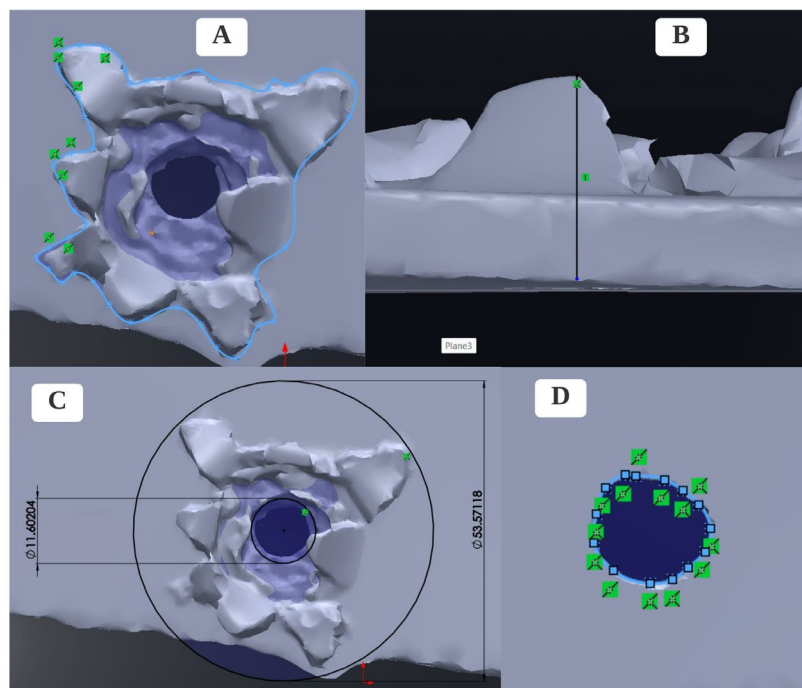
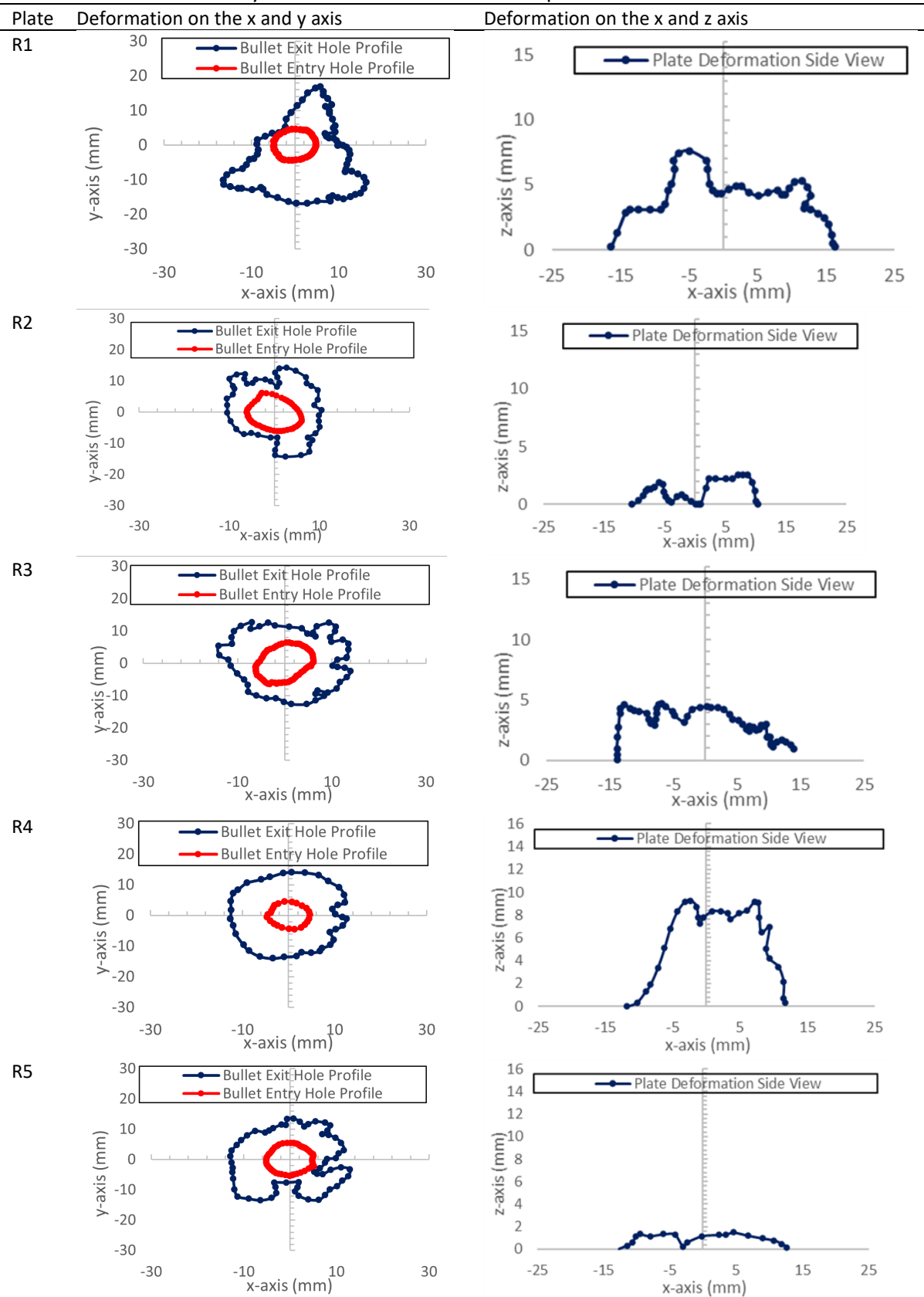


Fig. 5. 3D scan deformation profile capture (A) Deformation profile of the exit wound (B) Maximum displacement of material in bullet direction (C) Bullet hole diameter and deformation zone (D) Deformation profile of the entry wound

Table 3
 Deformation Profile of Recycled AA6061 Plates for Each Impact Event



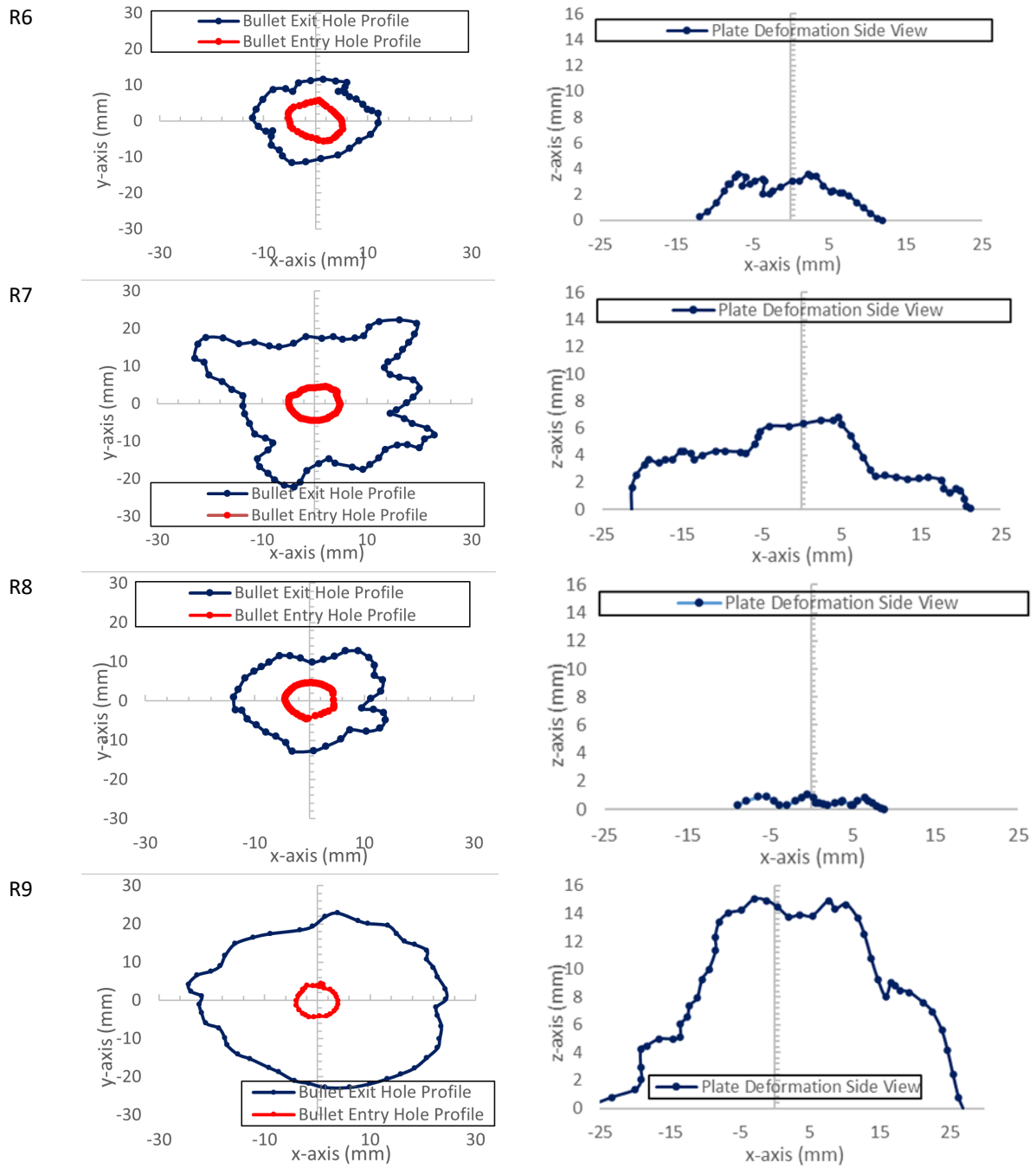


Table 4
 Characterized Parameter Values for Each Impact Event

Plate Designation	Bullet Entry Hole Area (mm ²)	Bullet Exit Hole Area (mm ²)	Impact Velocity (m/s)	Residual Velocity (m/s)	Maximum Deformation Length (z-axis) (mm)
R1	70	533	308	180	7.62
R2	105	411	333	230	3
R3	110	477	402	241	4.84
R4	61	559	121	21	9.37
R5	83	489	308	177	1.77
R6	83	399	402	265	3.65
R7	69	1144	136	60	6.6
R8	62	514	308	142	1.1
R9	51	1693	389	101	15.35

3.1.1 Velocity changes

In this section the effect of the change in the velocity of the bullet while keeping the plate thickness constant on the deformation profile of the plates is investigated. It can be observed that while keeping the plate thickness constant and increasing bullet velocity, the deformation zone around the bullet hole seems to be decreasing in size. This can be explained in the context of the contact time between the bullet and the target plate. When the bullet has a lower velocity (lower strain rate), the contact time between the bullet and the target is longer, which leads to a more significant amount of its energy being absorbed by the target plate. This energy is then transformed from kinetic energy to the plastic deformation of the plate. Whereas, a bullet with higher impact velocities has a lower contact time leading to lower energy absorption by the plate and more localized deformation. In other words, as the bullet velocity is increased, the bullet loses its energy to the plate to a lesser extent as evidenced by observing the residual velocity of the bullet [39]. This can be seen vividly when comparing the surface areas of the deformation zones of the plates as seen in Figure 6. A clear decrease in deformation area is observed with increasing impact velocity for 4 and 5mm plates, where a deviation is observed in 3mm plates where the deformation area at 402 m/s is higher than at 333 m/s. This deviation can be attributed to oblique impact as seen in Table 3, the bullet entry hole profile of this particular impact event is elliptical instead of circular suggesting an oblique impact occurred. Oblique impacts have different mechanisms/trends compared to perfect-hit events. Thus, the break in trend can be attributed to oblique impact. The trend could be better defined with a wider range of impact velocity data.

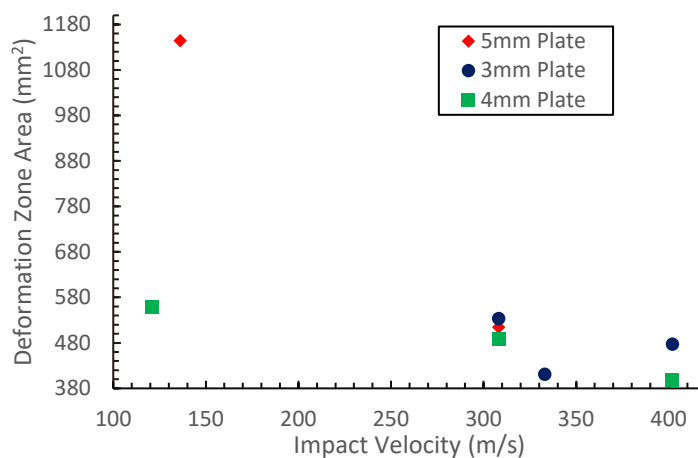


Fig. 6. Deformation zone area vs. Impact velocity graph for all impact events

Additionally, when observing Figure 7, it can be seen that the maximum deformation length at the back of the target plates follows an irregular trend with a change in velocity. For 3mm plates, the maximum deformation length is seen to be decreasing at first when going from 303 m/s to 333 m/s and then jumping up with a subsequent increase to 402 m/s. A similar trend is observed for 4mm plates when going from 121 m/s to 308 m/s and finally to 402 m/s. The deformation zone decreasing in area with an increase in impact velocity makes sense. It is already established, that higher impact velocity leads to more localized deformation around the impact area. In addition, higher velocity means higher energy. This combined with the localization of the stress results in the material being ejected from the plate by the bullet as it passes through at high velocity resulting in lesser deformation at the back of the plate.

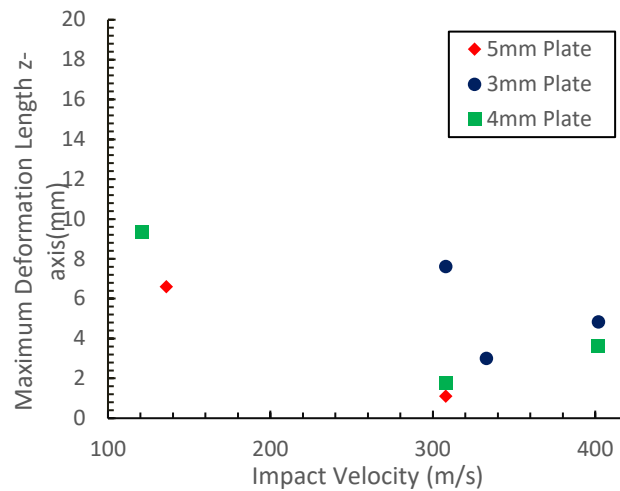


Fig. 7. Maximum Deformation (z-axis) vs. impact velocity graph for all impact events

3.1.2 Plate thickness

In this section, the effect of change in plate thickness while keeping the bullet velocity constant on the deformation profile of the plates is discussed.

Figure 8 shows the bullet exit hole surface area with respect to plate thickness. At the velocity of 402 m/s, a clear trend can be seen when going from 3mm to 4mm plate thickness. The deformation zone gets smaller as the thickness is increased. At 308 m/s same observation can be made when going from 3 to 4mm. however, when going from 4mm to 5mm plate thickness an increase in the deformation zone is observed.

On the other hand, it can be observed that the displacement of material along the direction of bullet travel changes with respect to the change in thickness of the target plates. Figure 9 shows that with an increase in the plate thickness, the maximum deformation length at the back of the plate decreases.

It is common knowledge that a thinner plate requires less energy for failure compared to a thicker plate [39,40]. When the bullet comes into contact with the plate, the plate experiences fracture faster if it is thinner. Because of this, the material at the back of the plate is displaced to the side fairly easily before it is ejected from the plate. Leading to a wider deformation zone and higher deformation length at the back of the plate. At higher thicknesses, more energy build-up is needed to cause failure, the material absorbs much more energy before it fails. Once failure occurs there is so much energy accumulated at the impact area that once it is released it causes the material in the bullet path to be ejected (instead of being displaced to the sides) from the base plate in the form of fragmentation. This leads to lower visible deformation at the back of the target plate after impact.

The analysis of the deformation profile of the recycled AA 6061 plates is crucial in establishing the behaviour and limits of the material undergoing failure. However, more data is required to fully catalogue its behaviour. For example, in this study, all of the impact events resulted in full penetration of the plates limiting the deformation behaviour analysis to only that after penetration. It is also interesting to investigate the deformation profile before penetration to study the damage progression. This will also allow investigation into the critical perforation velocity of the plates. The test setup utilized in this study is also prone to oblique impacts which hinder characterization. The bullet shape can be adjusted to a sphere to eliminate the possibility of oblique impacts. Furthermore,

the bullet mass has proven to be too much for the recycled AA6061 plates as it results in penetration even at low velocities. Lower mass bullets may prove to be stoppable by the plates.

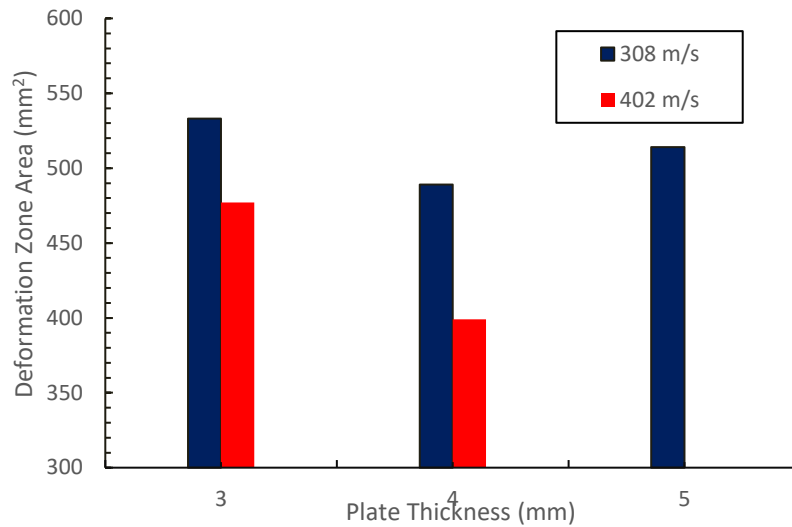


Fig. 8. Deformation zone area vs. plate thickness for all plates at two velocities

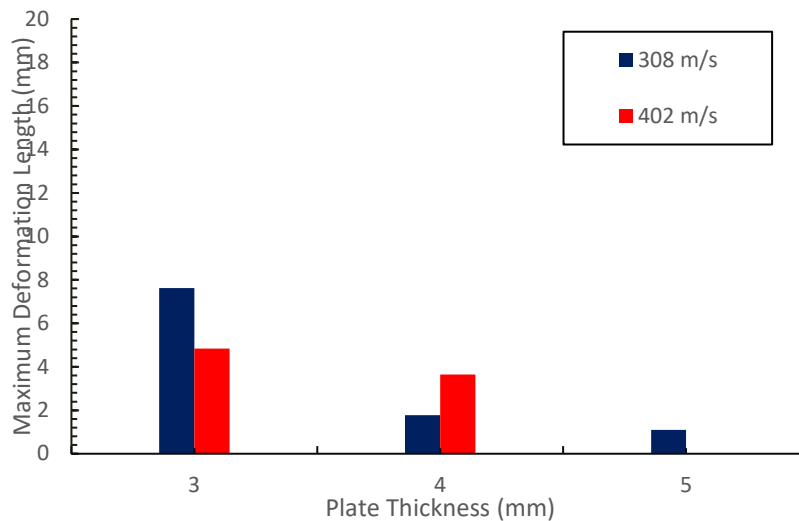


Fig. 9. Maximum deformation (z-axis) vs. Plate thickness for all plates at two velocities

3.2 Perforation Behaviour

The deformation profile of a material is no doubt influenced by its perforation behaviour and vice-versa. The perforation behaviour can be observed by visual inspection of the plates. In general, the recycled plates show a mixture of ductile and brittle behaviours. In this section, the perforation behaviour of the recycled AA6061 plates is discussed.

Petal formation is observed in impact events such as R1, R3, R4, R7, and R8. Figure 10 shows an instance of the type of petal formation observed. Petalling is a feature usually equated to ductile materials. The primary form of AA 6061 exhibits petal formation as well [41]. Petals usually form due to radial cracks and are observed when ogival or hemispherical bullets are used. The petals observed in recycled AA6061 plates are formed with material around the end of the bullet exit hole. The petals

in ductile materials mostly are initiated from the entry hole (accompanied by ductile hole growth). However, no such behaviour was observed for the recycled plates, suggesting that these plates are not fully ductile which is to be expected from directly recycled material. Impact events at lower impact velocities tend to result in petal formation.

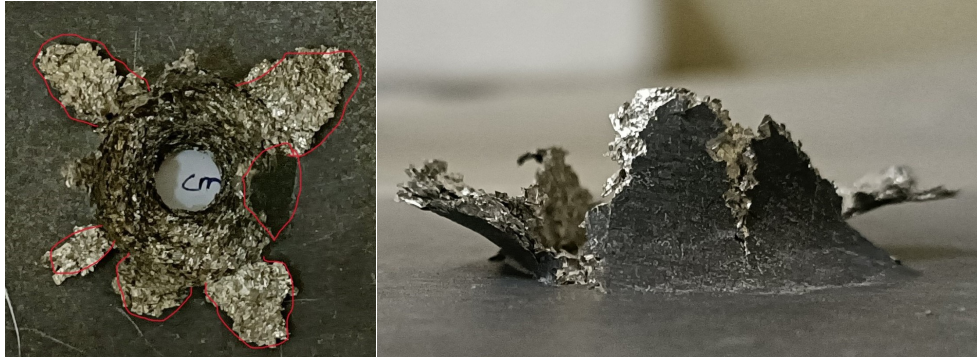


Fig. 10. Petal formation in recycled AA-6061 plates post impact

Plugging is also observed in some cases such as R6 where the bullet pushes the material out with it in the form of the bullet. Plugging is another characteristic of ductile materials. However, the plugs as seen in Figure 11, are not completely ductile in nature. The plugs are formed from poorly bonded together chips. It would be more accurate to describe it as a clump of fragments. This less-than-ductile behaviour is once again showing signs of mild ductility where the material exhibits signs of ductility but to a lower extent.



Fig. 11. Plug formation in recycled AA-6061 plates post impact

On the other hand, signs of brittle failure are also observed. Behaviours such as fragmentation are observed in almost all the impact events to some extent. Varying in sizes according to the plate thickness. Such as R8 having bigger fragments compared to R5. The material in and around the bullet impact area is ejected out in the form of chips or fragments as shown in Figure 12 below. Fragmentation is an inherent characteristic of brittle materials such as concrete [39,42]. AA 6061 by its nature is a ductile material. However, when directly recycled, the material loses its ductility due to improper chip bonding. This, in turn, results in some brittle behaviours being inherited by the recycled AA 6061 plates. This, however, does not equate to the material being completely brittle in its behaviour. In addition to the signs of ductility shown and discussed above, the brittle behaviour

of the recycled plates is also mild. In brittle materials, the material is also ejected towards the barrel (through the bullet entry hole) [42]. This, however, is not the case for recycled AA 6061 plates.

Brittle materials are also known to exhibit cone-shaped fractures where the size of the bullet exit hole crater is significantly bigger than the entry hole crater. Impact events for plates of higher thickness such as R9 show conal fracture as seen in Figure 13. In fully brittle materials no petals are observed as the matter is ejected instead. However, in the recycled AA 6061 plates conal fracture is accompanied by petals.

The recycled AA 6061 plates show a wide variety of perforation behaviour ranging from ductile to brittle when subjected to high-velocity impacts. It would be difficult to say which mode of failure is the dominant one without microstructural assessment such as fractography of the plates. The data available in this study is also limited to post-penetration. Investigating the deformation behaviour of the recycled AA 6061 plates will also help make a more educated assessment of the mode of failure. Still, there is no doubt the presence of both ductile and brittle behaviour is present.



Fig. 12. Fragmentation in recycled AA-6061 plates post impact

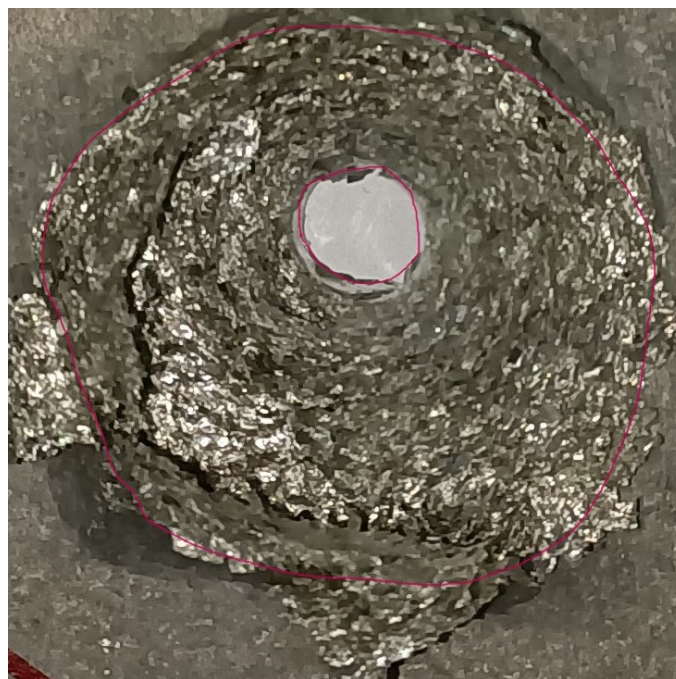


Fig. 13. Conal Fracture in recycled AA-6061 plates post impact

3.3 Velocity and Energy Analyses

This section deals with analysis related to the residual velocity of the impactor and energy absorption of the target plates with respect to impact velocity.

3.3.1 Residual velocity

Figure 14 shows the residual velocity versus impact velocity of each impact event. An almost linear relationship is observed between impact velocity and the residual velocity of the recycled AA6061 plates. An increase in residual velocity is observed with an increase in the impact velocity for all thicknesses. This means that the faster the bullet is, the more it retains its initial kinetic energy after passing through the target. From Figure 14, it can also be seen that at the same impact velocity plates of higher thickness will result in a lower residual velocity of the bullet. Take for example the velocity of 308 m/s where the residual velocity value drops from 180 m/s for 3mm plate to 177 m/s for 4mm plate and finally to 142 m/s for 5mm. Any variation in this trend is due to oblique impacts. This has been explained above, as thicker plates absorb more of the bullet's kinetic energy. It should also be noted that the difference in the residual velocity of the 3mm plate and 4mm plate is minimal 3 – 24 m/s. Similarly, for 4 and 5-mm plates, the difference is 35 m/s. As we can expect the trend of residual velocity getting lower with increasing thickness to be intact, for the sake of efficiency, the difference in residual velocity of plates of thickness varied by 1mm may be considered negligible.

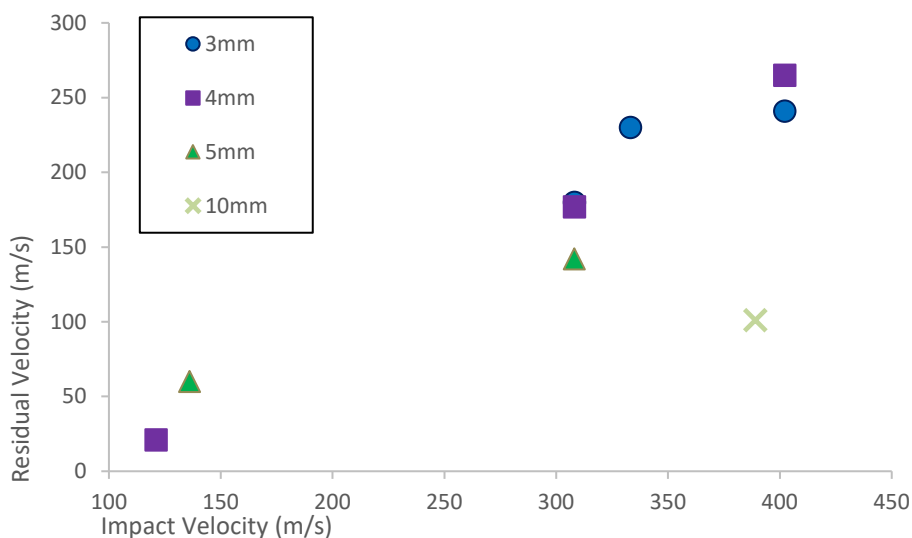


Fig. 14. Residual velocity vs. impact velocity of impact events

3.3.2 Energy absorption

Figure 15 shows the percentage amount of energy absorbed by the recycled AA6061 plates in each impact event against the residual velocity. Lower velocity impacts led to more of the impact energy being absorbed by the plates. Naturally, impacts with low residual velocities resulted in high energy absorption. Take for example samples R4, R5, and R6 (all plates of 4mm thickness) each having an impact velocity of 121 m/s, 308 m/s and 402 m/s. The energy absorption percentage decreased from 97% to 67% and finally to 57% respectively as the velocity increased. Smaller plate thicknesses have a lower amount of energy absorbed, which tracks as the bullet has to travel through a low

amount of material as the thickness is lowered. Hence it loses less of its energy to the plate. This can be confirmed by observing the energy absorbed for the R1, R5, and R8 where thickness is increased from 3mm to 4mm and 5mm and the velocity is kept at 308 m/s. The energy absorption increases from 66% to 67% and 79% respectively. The difference in energy absorption capability between the 3mm and 4 mm plates is observed to be insignificant.

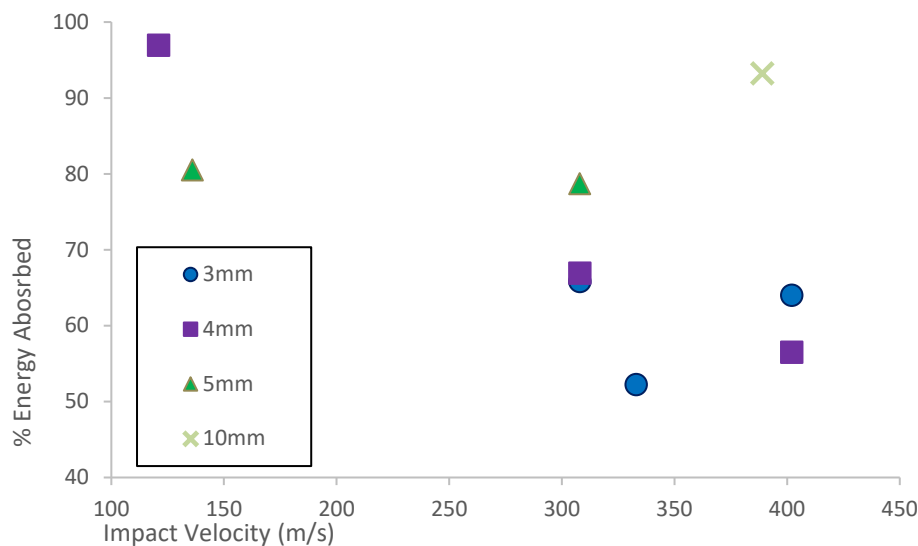


Fig. 15. % Energy absorbed vs. residual velocity of each test event

3. Conclusions

This study aimed to quantitatively characterize the deformation profile of the direct recycled AA 6061 plates. Additionally, the perforation behaviour of the plates along with some discussion on the residual velocity and energy absorption were also included. All this was achieved by testing multiple thicknesses of recycled plates with high-velocity impacts using a single-stage gas gun.

In total, 9 successful impact events were carried out. Their deformation profile was captured by 3D scans followed by dimensional analysis. The deformation profiles in some cases were observed to be non-axis-symmetrical. In some cases, signs of axis symmetry in one of the axes were observed as well. However, the anisotropy of the material may have been exaggerated due to some oblique impacts.

Next, the variation in the deformation profiles of the recycled AA 6061 plates with respect to changes in impact velocity and plate thickness were studied. It was observed that the deformation zone area decreased in size when the impact velocity was increased for a set thickness of the plate. This behaviour is attributed to lower contact times between the plate and the bullet at lower plate thickness. A similar trend is observed when investigating the change in maximum plate deformation at the back side of the plate, where the length of deformation decreases with a decrease in impact velocity. At higher velocity, the plate is subjected to higher energy in a more localized region which results in material ejection from the plate as opposed to displacement.

Variation in deformation profile with change in plate thickness was also studied. The deformation zone was observed to be more localised (smaller) for thicker plates. The maximum deformation length at the back of the plate also follows the same trend. This is due to the fact the thinner plates require lesser amounts of energy to fracture, leading to the occurrence of fracture at the early stage of contact with the bullet. The material is displaced to the sides of the bullet hole before it can be

completely severed and ejected by the bullet leading to more visible deformation at the back of the plate. Thus, thicker plates exhibit more fragmentation compared to thinner plates.

The perforation behaviour of the plates was investigated next. The material shows signs of ductile fractures such as petal and plug formation, along with brittle features such as fragmentation, and conal fractures. The materials seem to be exhibiting both ductile and brittle features, which can be explained by the nature of the recycling process. Both the perforation behaviour and the deformation profile could be further elaborated upon with the use of microstructural analysis.

Residual velocity was observed to increase with an increase in impact velocity and decrease with an increase in plate thickness. The same trend is observed with an increase in plate thickness.

Overall, the material shows a mix of ductile and brittle fracture modes. Throughout the study, however, an oblique impact caused a lot of hindrance in the observation and characterization of the deformation behaviour under impact loading. The test setup utilized tends to produce the oblique impact which is hard to avoid without significant alterations to the setup itself such as rifling the gun barrel. It is observed that the bullet shape contributes towards this issue. In addition, all of the impact events (even at low-velocity events) experienced a complete penetration. Therefore, no information was attained on the deformation behaviour of the material before a complete penetration. This is crucial information in the perforation behaviour characterization. In future research, a lower-mass bullet with a spherical shape can be adopted as a potential replacement to avoid the above issues. These criteria can be regarded as a better option to explore the perforation behaviour of such recycled materials since more work is needed to further establish the understanding.

Acknowledgement

The authors wish to convey sincere gratitude to the Ministry of Higher Education Malaysia (MOHE) for providing the financial means during the preparation to complete this work under the Fundamental Research Grant Scheme (FRGS/1/2020/TK02/UTHM/02/5), FRGS Vot K331.

References

- [1] Bringezu, Stefan, Anu Ramaswami, Heinz Schandl, Megan O'Brien, Rylie E. Pelton, and Ajay S. Nagpure. "Assessing global resource use: A systems approach to resource efficiency and pollution reduction." (2017).
- [2] Meshram, Arunabh, Rohit Jha, and Seby Varghese. "Towards recycling: Understanding the modern approach to recover waste aluminium dross." *Materials Today: Proceedings* 46 (2021): 1487-1491. <https://doi.org/10.1016/j.matpr.2020.11.423>
- [3] Wong, David S., and Pascal Lavoie. "Aluminum: recycling and environmental footprint." *Jom* 71, no. 9 (2019): 2926-2927. <https://doi.org/10.1007/s11837-019-03656-9>
- [4] Milovanoff, Alexandre, I. Daniel Posen, and Heather L. MacLean. "Quantifying environmental impacts of primary aluminum ingot production and consumption: A trade-linked multilevel life cycle assessment." *Journal of Industrial Ecology* 25, no. 1 (2021): 67-78. <https://doi.org/10.1111/jiec.13051>
- [5] Baffari, Dario, Gianluca Buffa, Giuseppe Ingarao, Attilio Masnata, and Livan Fratini. "Aluminium sheet metal scrap recycling through friction consolidation." *Procedia Manufacturing* 29 (2019): 560-566. <https://doi.org/10.1016/j.promfg.2019.02.134>
- [6] Brough, Daniel, and Hussam Jouhara. "The aluminium industry: A review on state-of-the-art technologies, environmental impacts and possibilities for waste heat recovery." *International Journal of Thermofluids* 1 (2020): 100007. <https://doi.org/10.1016/j.ijft.2019.100007>
- [7] Kore, A. S., K. C. Nayak, and P. P. Date. "Formability of aluminium sheets manufactured by solid state recycling." In *Journal of Physics: Conference Series*, vol. 896, no. 1, p. 012007. IOP Publishing, 2017. <https://doi.org/10.1088/1742-6596/896/1/012007>
- [8] Ahmad, A., M. A. Lajis, N. K. Yusuf, and A. Wagiman. "Hot press forging as the direct recycling technique of aluminium—A review." *ARPJ J. Eng. Appl. Sci* 11, no. 4 (2016): 2258-2265.
- [9] Ho, C. S., and M. K. Mohd Nor. "An experimental investigation on the deformation behaviour of recycled aluminium alloy AA6061 undergoing finite strain deformation." *Metals and Materials International* 27 (2021): 4967-4983. <https://doi.org/10.1007/s12540-020-00858-8>

- [10] Ho, Choon Sin, Muhamad Afandi Ab Rani, Mohd Khir Mohd Nor, Norzarina Ma'at, Mohamed Thariq Haji Hameed Sultan, Mohd Amri Lajis, and Nur Kamilah Yusuf. "Characterization of anisotropic damage behaviour of recycled aluminium alloys AA6061 undergoing high velocity impact." *International Journal of Integrated Engineering* 11, no. 1 (2019).
- [11] Ahmad, Azlan, Mohd Amri Lajis, and Nur Kamilah Yusuf. "On the role of processing parameters in Producing recycled aluminum AA6061 based metal matrix composite (MMC-AIR) prepared using hot press forging (HPF) process." *Materials* 10, no. 9 (2017): 1098. <https://doi.org/10.3390/ma10091098>
- [12] Khamis, S. S., M. A. Lajis, and R. A. O. Albert. "A sustainable direct recycling of aluminum chip (AA6061) in hot press forging employing response surface methodology." *Procedia CIRP* 26 (2015): 477-481. <https://doi.org/10.1016/j.procir.2014.07.023>
- [13] Wagiman, Abdullah, Mohammad Sukri Mustapa, Shazarel Shamsudin, Mohd Amri Lajis, Rosli Asmawi, Mohammed H. Rady, and Mohd Shahir Yahya. "Effect of Thermally-Treated Chips on Density of AlMgSi Alloys Recycled Using Solid-State Technique." *Processes* 8, no. 11 (2020): 1406. <https://doi.org/10.3390/pr8111406>
- [14] Chiba, Ryoichi, Tamon Nakamura, and Mitsutoshi Kuroda. "Solid-state recycling of aluminium alloy swarf through cold profile extrusion and cold rolling." *Journal of Materials Processing Technology* 211, no. 11 (2011): 1878-1887. <https://doi.org/10.1016/j.jmatprotec.2011.06.010>
- [15] Gronostajski, J. Z., H. Marciniak, and A. Matuszak. "Production of composites on the base of AlCu4 alloy chips." *Journal of materials processing technology* 60, no. 1-4 (1996): 719-722. [https://doi.org/10.1016/0924-0136\(96\)02410-7](https://doi.org/10.1016/0924-0136(96)02410-7)
- [16] Gronostajski, J., H. Marciniak, and A. Matuszak. "New methods of aluminium and aluminium-alloy chips recycling." *Journal of materials processing technology* 106, no. 1-3 (2000): 34-39. [https://doi.org/10.1016/S0924-0136\(00\)00634-8](https://doi.org/10.1016/S0924-0136(00)00634-8)
- [17] Rady, Mohammed Hussien, Mohammad Sukri Mustapa, Mohd Azhar Harimon, Mustaffa R. Ibrahim, S. Shamsudin, Mohd Amri Lajis, Abdullah Wagiman, Muntadher S. Msebawi, and Farazila Yusof. "Effect of hot extrusion parameters on microhardness and microstructure in direct recycling of aluminium chips." *Materialwissenschaft und Werkstofftechnik* 50, no. 6 (2019): 718-723. <https://doi.org/10.1002/mawe.201800214>
- [18] Yusuf, Nur Kamilah, Mohd Amri Lajis, and Azlan Ahmad. "Multiresponse optimization and environmental analysis in direct recycling hot press forging of aluminum AA6061." *Materials* 12, no. 12 (2019): 1918. <https://doi.org/10.3390/ma12121918>
- [19] Rady, Mohammed Hussein, Mohammad Sukri Mustapa, Abdullah Wagiman, Sami Al-Alimi, Shazarel Shamsudin, Mohd Amri Lajis, Mohamad Norani Mansor, and Mohd Azhar Harimon. "Effect of the heat treatment on mechanical and physical properties of direct recycled aluminium alloy (AA6061)." *International Journal of Integrated Engineering* 12, no. 3 (2020): 82-89.
- [20] Wan, Bingbing, Weiping Chen, Tiwen Lu, Fangfang Liu, Zhenfei Jiang, and Mengdi Mao. "Review of solid state recycling of aluminum chips." *Resources, Conservation and Recycling* 125 (2017): 37-47. <https://doi.org/10.1016/j.resconrec.2017.06.004>
- [21] Ho, C. S., and M. K. Mohd Nor. "Tensile behaviour and damage characteristic of recycled aluminium alloys AA6061 undergoing finite strain deformation." *Proceedings of the Institution of Mechanical Engineers, Part C: Journal of Mechanical Engineering Science* 235, no. 12 (2021): 2276-2284. <https://doi.org/10.1177/0954406220950349>
- [22] Ho, C. S., and M. K. Mohd Nor. "An experimental investigation on the deformation behaviour of recycled aluminium alloy AA6061 undergoing finite strain deformation." *Metals and Materials International* 27 (2021): 4967-4983. <https://doi.org/10.1007/s12540-020-00858-8>
- [23] Ma'at, Norzarina, Mohd KhirMohd Nor, Choon Sin Ho, Noradila Abdul Latif, Kamarul-Azhar Kamarudin, Saifulnizan Jamian, Mohd Norihan Ibrahim, and Muhamad Khairudin Awang. "Effects of temperatures and strain rate on the mechanical behaviour of commercial aluminium alloy AA6061." *Journal of Advanced Research in Fluid Mechanics and Thermal Sciences* 54, no. 1 (2019): 21-26.
- [24] Mohd Nor, Mohd Khir, and Ibrahim Mohamad Suhaimi. "Effects of temperature and strain rate on commercial aluminum alloy AA5083." *Applied Mechanics and Materials* 660 (2014): 332-336. <https://doi.org/10.4028/www.scientific.net/AMM.660.332>
- [25] Ho, C. S., MK Mohd Nor, M. A. Ab Rani, N. Ma'at, MT Hameed Sultan, and M. A. Lajis. "Plastic anisotropic and damage evolution analysis of recycled aluminium alloy AA6061 at high rate of strain." *Journal of Mechanical Engineering and Sciences* 14, no. 4 (2020): 7589-7599. <https://doi.org/10.15282/jmes.14.4.2020.23.0597>
- [26] Mohd Nor, Mohd Khir, Rade Vignjevic, and James Campbell. "Plane-stress analysis of the new stress tensor decomposition." *Applied Mechanics and Materials* 315 (2013): 635-639. <https://doi.org/10.4028/www.scientific.net/AMM.315.635>
- [27] Nor, MK Mohd. "Modeling of constitutive model to predict the deformation behaviour of commercial aluminum alloy AA7010 subjected to high velocity impacts." *ARPN J. Eng. Appl. Sci* 11, no. 4 (2016): 2349-2353.

- [28] Mohd Nor, M. K., C. S. Ho, N. Ma'at, and M. F. Kamarulzaman. "Modelling shock waves in composite materials using generalised orthotropic pressure." *Continuum mechanics and thermodynamics* 32 (2020): 1217-1229. <https://doi.org/10.1007/s00161-019-00835-6>
- [29] Ismail, A. E., S. H. Masran, S. Jamian, K. A. Kamarudin, MK Mohd Nor, NH Muhd Nor, AL Mohd Tobi, and M. K. Awang. "Fracture toughness of woven kenaf fibre reinforced composites." In *IOP Conference Series: Materials Science and Engineering*, vol. 160, no. 1, p. 012020. IOP Publishing, 2016. <https://doi.org/10.1088/1757-899X/160/1/012020>
- [30] Mohd Nor, M. K., N. Ma'at, and C. S. Ho. "An anisotropic elastoplastic constitutive formulation generalised for orthotropic materials." *Continuum Mechanics and Thermodynamics* 30 (2018): 825-860. <https://doi.org/10.1007/s00161-018-0645-7>
- [31] Rahman, Muhammad Faisal Abdul, Kamarul Azhar Kamarudin, Hendery Dahlan, and Mohamed Nasrul Mohamed Hatta. "Ballistic Limit Prediction On Nacre Shell Using Numerical Simulation Approach." *Advanced Research in Natural Fibers* 2, no. 1 (2020): 25-29.
- [32] Zahrin, Muhammad Fadhli, Kamarul-Azhar Kamarudin, and Ahmad Sufian Abdullah. "Numerical simulation of oblique impact on structure using finite element method." In *AIP Conference Proceedings*, vol. 2644, no. 1. AIP Publishing, 2022. <https://doi.org/10.1063/5.0106753>
- [33] Kamarudin, Kamarul Azhar, and Iskandar Abdul Hamid. "Effect of high velocity ballistic impact on pretensioned carbon fibre reinforced plastic (CFRP) plates." In *IOP conference series: materials science and engineering*, vol. 165, no. 1, p. 012005. Iop Publishing, 2017. <https://doi.org/10.1088/1757-899X/165/1/012005>
- [34] Ariffin, Nuruddin, Kamarul-Azhar Kamarudin, Ahmad Sufian Abdullah, and Mohd Idrus Abd Samad. "Crash Investigation on Frontal Vehicle Chassis Frame using Finite Element Simulation." *Journal of Advanced Research in Applied Sciences and Engineering Technology* 28, no. 2 (2022): 124-134. <https://doi.org/10.37934/araset.28.2.124134>
- [35] Nor, MK Mohd. "Modelling inelastic behaviour of orthotropic metals in a unique alignment of deviatoric plane within the stress space." *International Journal of Non-Linear Mechanics* 87 (2016): 43-57. <https://doi.org/10.1016/j.ijnonlinmec.2016.09.011>
- [36] Mohd Nor, Mohd Khir, and Muhammad Zulhusmi Dol Baharin. "Rollover analysis of heavy vehicle bus." *Applied Mechanics and Materials* 660 (2014): 633-636. <https://doi.org/10.4028/www.scientific.net/AMM.660.633>
- [37] Kadhim, M. H., N. A. Latif, M. A. Harimon, A. A. Shamran, and D. R. Abbas. "Effects of side-groove and loading rate on the fracture properties of aluminium alloy AL-6061." *Materialwissenschaft und Werkstofftechnik* 51, no. 6 (2020): 758-765. <https://doi.org/10.1002/mawe.201900262>
- [38] Bendarma, Amine, Alexis Rusinek, Tomasz Jankowiak, Tomasz Lodygowski, and Bin Jia. "Experimental analysis of the aluminum alloy sheet subjected to impact and perforation process." *Materials Today: Proceedings* 36 (2021): 88-93. <https://doi.org/10.1016/j.matpr.2020.05.408>
- [39] Safri, S. N. A., M. T. H. Sultan, Noorfaizal Yidris, and Faizal Mustapha. "Low velocity and high velocity impact test on composite materials—a review." *Int. J. Eng. Sci* 3, no. 9 (2014): 50-60.
- [40] Nassir, Nassier A., and Ayad K. Hassan. "Numerical response of aluminium plate (6061-T6) under dynamic loadings." In *IOP Conference Series: Materials Science and Engineering*, vol. 1076, no. 1, p. 012076. IOP Publishing, 2021. <https://doi.org/10.1088/1757-899X/1076/1/012076>
- [41] Dubey, R., R. Jayaganthan, D. Ruan, N. K. Gupta, N. Jones, and R. Velmurugan. "Ballistic perforation and penetration of 6xxx-series aluminium alloys: A review." *International Journal of Impact Engineering* 172 (2023): 104426. <https://doi.org/10.1016/j.ijimpeng.2022.104426>
- [42] Kristoffersen, Martin, Oda L. Toreskås, Sumita Dey, and Tore Børvik. "Ballistic perforation resistance of thin concrete slabs impacted by ogive-nose steel projectiles." *International Journal of Impact Engineering* 156 (2021): 103957. <https://doi.org/10.1016/j.ijimpeng.2021.103957>
- [43] Kamarudin, Kamarul Azhar, Mohamed Nasrul Mohamed Hatta, Ranjhini Anpalagan, Noor Wahida Ab Baba, Mohd Khir Mohd Noor, Rosniza Hussin, and Ahmad Sufian Abdullah. "Seashell structure under binder influence." *Journal of Advanced Research in Fluid Mechanics and Thermal Sciences* 46, no. 1 (2018): 122-128.